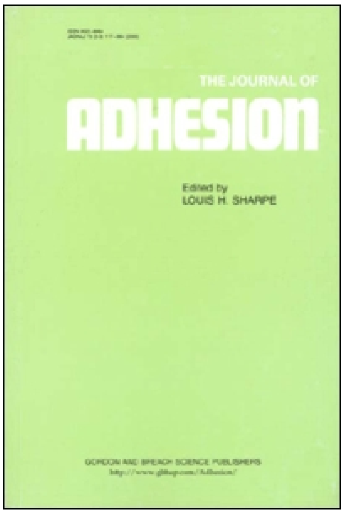

The Journal of Adhesion
Publication details, including instructions for authors and subscription information:
http://www.informaworld.com/smpp/title~content=t713453635

Bonding and Debonding Processes in Tack of Pressure-Sensitive Adhesives

Toshihide Tsukatani[a]; Yasunori Hatano[a]; Hiroshi Mizumachi[a]
[a] Laboratory of Chemistry of Polymer Materials, Department of Forest Products, Faculty of Agriculture, The University of Tokyo, Bunkyo-ku, Tokyo, Japan

To cite this Article Tsukatani, Toshihide , Hatano, Yasunori and Mizumachi, Hiroshi(1989) 'Bonding and Debonding Processes in Tack of Pressure-Sensitive Adhesives', The Journal of Adhesion, 31: 1, 59 — 71
To link to this Article: DOI: 10.1080/00218468908048214
URL: http://dx.doi.org/10.1080/00218468908048214

J. Adhesion, 1989, Vol. 31, pp. 59–71
Reprints available directly from the publisher
Photocopying permitted by license only

Printed in the United Kingdom

Bonding and Debonding Processes in Tack of Pressure-Sensitive Adhesives†

TOSHIHIDE TSUKATANI, YASUNORI HATANO and HIROSHI MIZUMACHI

Laboratory of Chemistry of Polymer Materials, Department of Forest Products, Faculty of Agriculture, The University of Tokyo, Bunkyo-ku, Tokyo 113, Japan

(Received February 6, 1989; in final form May 8, 1989)

Rolling friction coefficient of two acrylic pressure sensitive adhesives (PSAs) are measured as a function of velocity at several temperatures. It is found that the time (or velocity)–temperature superposition procedure is applicable for one PSA, while it is not for the other. The authors came to the conclusion that the rate of increase of the true contact area is different for the two adhesives. The time–temperature superposition is possible only in the case where the activation energy of the bonding process is equal to that of the debonding process.

KEY WORDS Pressure sensitive adhesives; pulling cylinder; rolling friction coefficient; bonding-process; debonding-process; probe tack; activation energy; time–temperature superposition.

INTRODUCTION

The authors[1–6] have pointed out the fact that tack of pressure-sensitive adhesives (PSAs) is closely related to the rolling friction coefficient f of the materials, and have evaluated f of various PSAs by means of both the rolling ball method and the pulling cylinder method. It has been clarified that by analysing the rolling motion of a ball on a PSA in the ordinary ball tack tests, we can evaluate f of the adhesive substantially in the velocity range of 10^1–10^2 cm/sec, but if we adopt the pulling cylinder method, we can measure f of the material over a much wider range of velocity. For a viscoelastic materials with tackiness, we generally find a peak or peaks at some velocity, and the peak(s) shifts toward the higher velocity side as the relaxation time of the material decreases, or vice versa.

Now, we have to think of the physical meaning or rolling friction of the tacky materials. When a cylinder (or a ball) rolls on a PSA, the bonding and debonding processes proceed simultaneously in the contacting region. The theory[5] which the authors have previously developed in order to describe f in terms of viscoelastic parameters of the adhesives involved the debonding process only, which means

---

† Presented at the Twelfth Annual Meeting of The Adhesion Society, Inc., Hilton Head Island, South Carolina, February 20–22, 1989.

that the bonding process was implicitly assumed to proceed instantaneously. However, it is well known that the bonding process is also time-dependent,[7–9] and so we have to take this factor into consideration in the theory of rolling friction of the adhesives. Recently, the authors have modified the theory so as to include not only the debonding process, but also the bonding process.[10]

In this paper, comparisons are made between the theoretical predictions and some experimental data. Also, it is examined whether the time (or velocity)–temperature superposition procedure is applicable to the rolling friction of the tacky materials or not.

EXPERIMENTAL

Materials

Two acrylic PSAs with almost the same chemical composition (Butyl Acrylate/Acrylic Acid = 90/10) and with the same molecular weight are used in this study. One (PSA-T) is supplied by Toyo Ink Manufacturing Co., Ltd. and the other (PSA-N) by Nichiban Co., Ltd. Both of them were sandwiched between the releasing papers, and the detailed information about the releasing agents for the two series of samples was not supplied. PSAs were transferred onto glass plates for measurements of f.

Measurement of f

The pulling cylinder method is employed to measure f of the PSAs. The apparatus used in this study is a rheometer CR-200D of Sun Scientific Co., Ltd. (San Kagaku), which is slightly modified. A cylinder made of brass is pulled on the PSAs at a constant velocity ranging from 10^{-4} to 10^{2} cm/sec, and in the temperature range from −25 to 45°C. In most cases, the force P to pull the cylinder was measured for its first revolution on the PSA at each velocity, because the value could be different for subsequent revolutions. However, when the velocity is extremely high (10 cm/sec), the first revolution was hardly distinguished from the other on the chart. For the PSAs under study, the interfacial failure occurred in that velocity region and the value of P did not vary greatly for some revolutions. So, the average for the first few rollings of the cylinder on the PSA surface was determined in these cases.

Values of f were calculated by the following equation:

$$f = PR/Mg \tag{1}$$

where R and M are radius and mass, respectively, of the cylinder.

Measurement of probe tack

In order to get the information on the bonding process, the probe tack was measured as a function of dwell time in the temperature range of 5–37°C, using

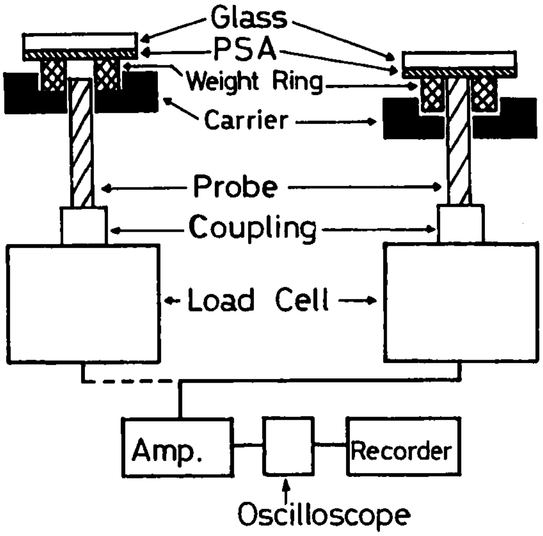

FIGURE 1 NS Probe Tack Tester.

an NS Probe Tack Tester of Nichiban Co., Ltd., a diagram of which is shown in Figure 1. Diameter of the stainless steel probe is 5 mm, and stress by the weight-ring is $100\,g/cm^2$. Moving speed of the probe is 1 cm/sec in every measurement.

RESULTS AND DISCUSSIONS

(A) Rolling friction coefficient

Figure 2 shows a plot of f against $\log v$ for PSA-T at several temperatures. We find two peaks, especially at higher temperatures. As the temperature of measurement is lowered, both peaks shift toward lower velocity region. Here, it is interesting to notice that the peak at the higher velocity side diminishes at lower temperatures. This means that the time (or velocity)–temperature superposition procedure is not applicable to the f *vs.* $\log v$ curves for this PSA. Nevertheless, we tried to reduce these curves to 20°C and got a "master curve" as shown in Figure 3. A part of the curve which corresponds to cohesive failure in the low velocity region at each temperature can be superposed, but the other part of the curve cannot. The Arrhenius plot of the shift factor a_T is shown in Figure 4, and the activation energy is about 19 kcal/mole. Figure 5 shows similar data for another acrylic PSA (PSA-N) at three different temperatures. Here again, we find two peaks at each temperature. However, the peak at the higher velocity side does not diminish for this PSA. This means that the time–temperature superposition procedure is apparently applicable to this material over the whole range, and the master curve is shown in Figure 6. The activation energy calculated from the

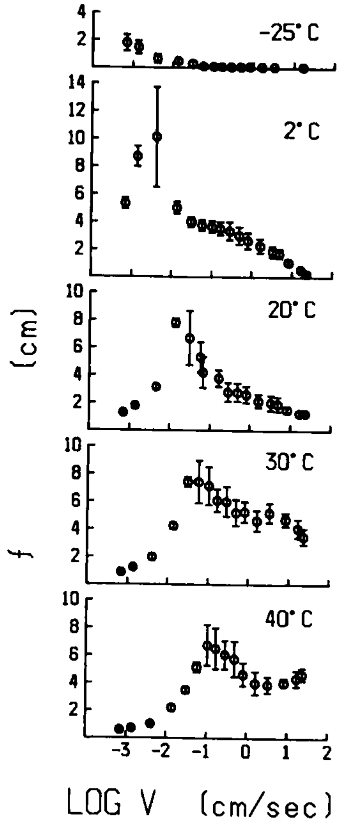

FIGURE 2 *f vs.* log *v* for PSA-T.

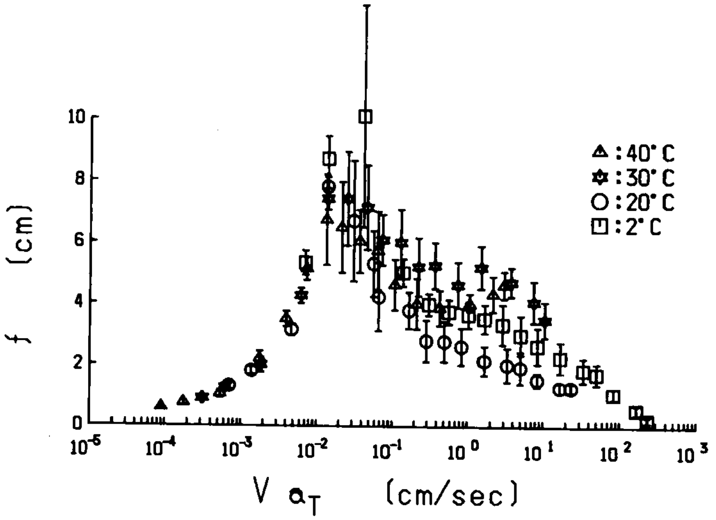

FIGURE 3 Master curve of *f* for PSA-T, reduced to 20°C.

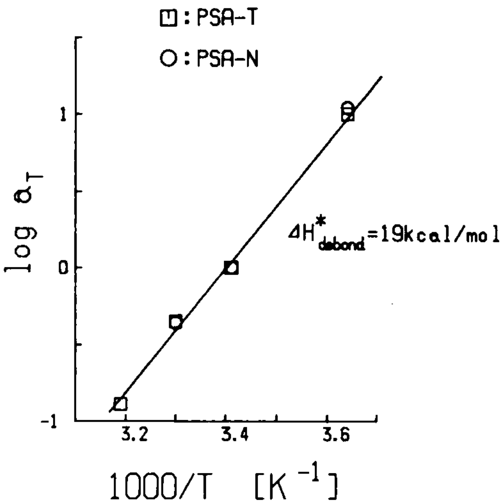

FIGURE 4 Arrehenius plot of the shift factor a_T for the lower velocity part of the curve of f vs. log v.

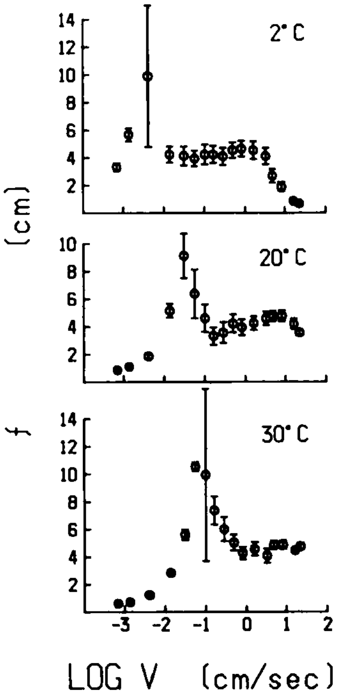

FIGURE 5 f vs. log v for PSA-N.

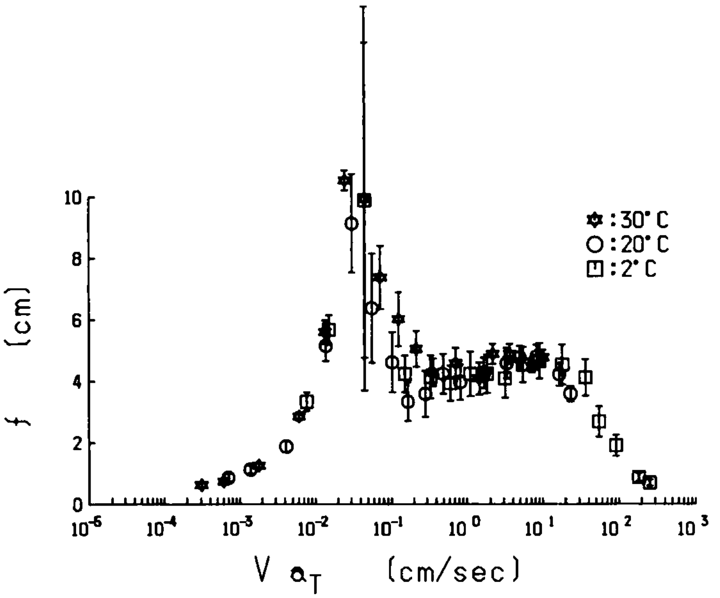

FIGURE 6 Master curve of f for PSA-N, reduced to 20°c.

Arrhenius plot of the shift factor a_T, which is also shown in Figure 4, is about 19 kcal/mole.

Now, we have to think of the reason why the f *vs.* $\log v$ curve of one PSA can be superposed in the whole velocity range, and that of the other cannot. The authors have derived a modified equation of f, taking into account both the bonding and debonding processes.

When a cylinder rolls on a PSA, it is pulled back by the extensional deformation of the PSA. The surface element shown in Figure 7 is $brd\theta$ in the case for which the bonding-process is instantaneous. On the other hand, in the case where the process is time-dependent, that element must be multiplied by a factor $a(t)$, which is the ratio of the true bonding area $A(t)$ at time t and that, $A(\infty)$, at infinite time, because time goes on from $\theta = 0(t = 0)$ to $\theta = \theta(t = t)$, where $t = R\theta/v$. So, the resulting equation is as follows;

$$f = \frac{R^2 b}{Mg} \int_0^{\theta_b} \sigma(\theta) a(R\theta/v) \cos\theta \sin\theta \, d\theta \tag{2}$$

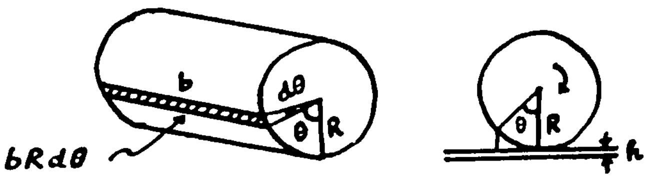

FIGURE 7 Rolling cylinder.

where $\sigma(\theta)$ is the stress generated by elongation of the PSA, which must be expressed as a function of θ, and θ_b is the angle where adhesive failure (cohesive and/or interfacial) is steadily taking place on the cylinder surface. W. M. Bright,[7] K. Kanamaru[8] and J. Furukawa[9] described the rate of increase of the effective contact area by a first-order rate equation. For this case, $a(t)$ or $a(R\theta/v)$ is given by the following equation ($n = 1$);

$$a(R\theta/v) = 1 - \left\{1 - \frac{A(0)}{A(\infty)}\right\} \exp(-kR\theta/v) \tag{3}$$

Of course, we can generalize it to the nth order rate equation ($n \neq 1$);

$$a(R\theta/v) = 1 - \left[\left\{1 - \frac{A(0)}{A(\infty)}\right\}^{-n+1} + (n-1)A(\infty)^{n-1}kR\theta/v\right]^{-1/(n-1)} \tag{4}$$

Here, k is the rate constant for the bonding process, or process of increasing contact area. If we adopt some mechanical model, we can derive $\sigma(\theta)$, and if we assume some failure criteria, we can determine θ_b.

It is well known that the time (or strain rate)–temperature superposition procedure can formally be applied to the stress and strain at break (σ_B, ε_B) of rubbers over a wide range, and the master curve can be obtained in spite of the fact that the phenomenon involves large deformation and failure, which is far from linearly viscoelastic. A plot of σ_B against ε_B gives a so-called "failure envelope," and it has a universal shape for the viscoelastic materials. T. Hata[11] has shown that the general features of the failure envelopes of viscoelastic materials can be qualitatively reproduced in a linear viscoelastic manner, adopting a simple mechanical model as shown in Figure 8, and assuming some failure criteria. For this case, $\delta(\theta)$ can be described as follows;

$$\sigma(\theta) = \sum_{i=1}^{2} \frac{E_i R}{h} \frac{1}{E_i^2 R^2/v^2\eta_i^2 + 1} \left(\frac{E_i R}{v\eta_i} \sin\theta - \cos\theta + e^{-(E_i R/v\eta_i)\theta}\right) \tag{5}$$

The failure criteria adopted are such that cohesive failure occurs either when the strain of the spring in the weak point (element 1) reaches a critical value (ε_{11c}) or when strain of the dashpot reaches another critical value (ε_{12c}). And in order to take interfacial failure into consideration, an additional failure criterion is needed. T. Hata[12] postulated that interfacial failure occurs when stored energy in the springs of the model reaches a critical value W_c. The failure criteria are

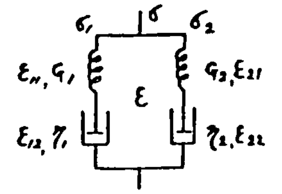

FIGURE 8 Two Maxwell elements in parallel connection.

expressed by the following equations;

$$\varepsilon_{11} = \frac{\sigma_1}{E_1} = \frac{R}{h} \frac{1}{E_1^2 R^2 / v^2 \eta_1^2 + 1} \left(\frac{E_1 R}{v \eta_1} \sin\theta - \cos\theta + e^{-(E_1 R / v \eta_1)\theta} \right) = \varepsilon_{11c} \tag{6}$$

$$\varepsilon_{12} = \frac{E_1 R^2}{h v \eta_1} \frac{1}{E_1^2 R^2 / v^2 \eta_1^2 + 1} \left[\frac{E_1 R}{v \eta_1} (1 - \cos\theta) - \sin\theta - \frac{v \eta_1}{E_1 R} (e^{-E_1 R / v \eta_1)\theta} - 1) \right] = \varepsilon_{12c} \tag{7}$$

$$W = \sum_{i=1}^{2} \tfrac{1}{2} \varepsilon_{i1}^2 E_i = \sum_{i=1}^{2} \frac{1}{2} \frac{\sigma_i^2}{E_i} = W_c \tag{8}$$

Then, we can numerically calculate f for the appropriate values of the parameters as a function of v, combining these equations. According to this theory, we can show that the curve shifts towards the higher velocity side as temperature increases (or as the relaxation time decreases), and vice versa.

It is quite natural that the bonding process has a remarkable effect on the shape of the curve of f *vs.* $\log v$, especially in the higher velocity region. Figure 9 shows some examples of the superposition of theoretical curves of f *vs.* $\log v$ in the case

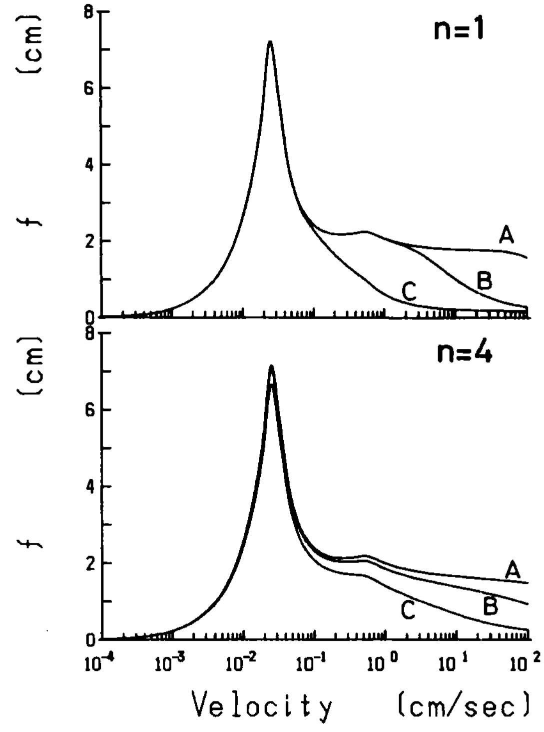

FIGURE 9 Superposition of the theoretical curves of f *vs.* $\log v$ in the case where $\Delta H^*_{\text{bond}} = 1.5 \times \Delta H^*_{\text{debond}}$. Values of the parameters are: $R = 0.5$ cm, $b = 2.5$ cm, Mg = 50000 dyne, $E_1 = E_2 = 10^{10}$ dyne/cm^2, $\varepsilon_{11c} = 0.1$, $\varepsilon_{12c} = 0.35$, $W_c = 7.0 \times 10^7$ erg/cm^3, $A(0)/A(\infty) = 0.1$, $\tau_1 = 0.1$, $\tau_2 = 0.01$, $k(n = 1) = 10^{4.5}$, $k(n = 4) = 10^{-5.0}$ for curve A, $\tau_1 = 1.0$, $\tau_2 = 0.1$, $k(n = 1) = 10^{3.0}$, $k(n = 4) = 10^{-6.5}$ for curve B, $\tau_1 = 10.0$, $\tau_2 = 1.0$, $k(n = 1) = 10^{1.5}$, $k(n = 4) = 10^{-8.0}$ for curve C.

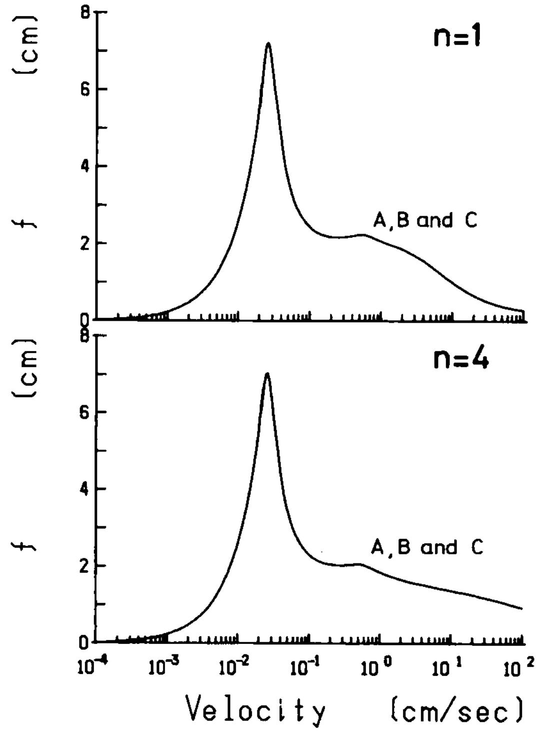

FIGURE 10 Superposition of the theoretical curves of f *vs.* $\log v$ in case where, $\Delta H^*_{\text{bond}} = \Delta H^*_{\text{debond}}$. Values of the parameters are: $\tau_1 = 0.1$, $\tau_2 = 0.01$, $k(n=1) = 10^4$, $k(n=4) = 10^{-5.5}$ for curve A, $\tau_1 = 1.0$, $\tau_2 = 0.1$, $k(n=1) = 10^3$, $k(n=4) = 10^{-6.5}$ for curve B, $\tau_1 = 10.0$, $\tau_2 = 1.0$, $k(n=1) = 10^2$, $k(n=4) = 10^{-7.5}$ for curve C. The remainder of the parameter values are the same as those given in Figure 9.

where the relaxation time τ_i of the mechanical model and the rate constant k of the bonding process have somewhat different temperature dependence. As we go from A (high temperature) to B (medium temperature), and then to C (low temperature) in Figure 9, τ_i increases by a factor of 10 each, and at the same time k decreases by a factor of $10^{1.5}$ each, which corresponds to the case where the activation energy ΔH^*_{bond} of the bonding process is 1.5 times larger than that $\Delta H^*_{\text{debond}}$ of the mechanical deformation which must be related to the debonding process. Then, the shape of the curve is partly the same (in the lower velocity side), but partly different (in the higher velocity side) at different temperatures, and in these cases the time–temperature superposition is not possible (or possible only in a restricted part). On the other hand, Figure 10 shows the superposition of theoretical curves of f *vs.* $\log v$ in the case where τ_i nad k have the same temperature dependence, or in other words $\Delta H^*_{\text{bond}} = \Delta H^*_{\text{debond}}$. In this case, the curve shifts along the $\log v$ axis, keeping the same shape when temperature is varied, and therefore the curves at different temperatures can be superposed over the whole range of velocity. Our conclusion, then, is that the difference between the master curves in Figure 3 and Figure 6 must be attributed to the difference between the bonding processes of the two PSAs.

(B) Probe tack

In order to elucidate the difference of bonding process of the two PSAs, the authors have studied the dependence of probe tack upon dwell time or time of contact of the probe and the PSA. Experimental data for PSA-T and PSA-N are shown in Figure 11 and Figure 12, respectively. In both cases, the probe tack value increases monotonously as a function of dwell time. This means the bonding process is obviously time-dependent. Photographs of the bonding part showed that very complicated phenomena are involved in this experiment, but the authors simply assume here that the probe tack value is proportional to the true contact area. There is considerable scatter of experimental points as shown in the Figures. These data are analysed by the least squares methods according to equation (3) and equation (4) with various n. The smallest deviation was seen when n is around 4, and the calculated curves for the 4th-order rate equation are also shown in the Figures. Physical meanings of the absolute values of the

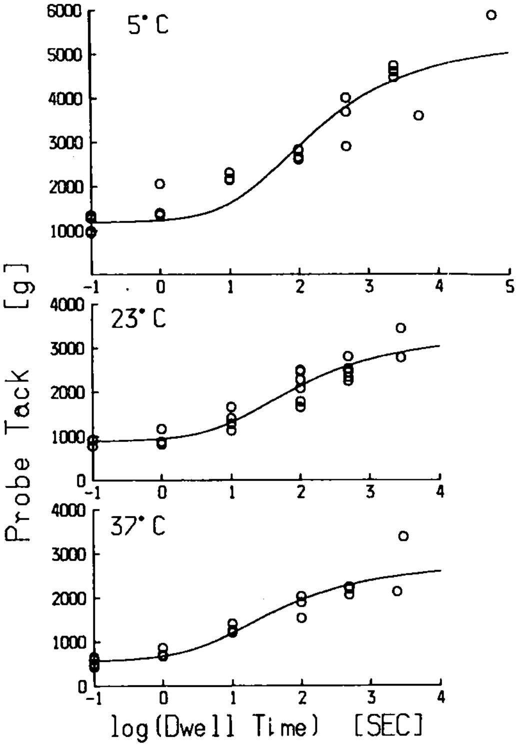

FIGURE 11 Probe track *vs.* dwell time for PSA-T. Solid line is a curve of the 4th order rate equation.

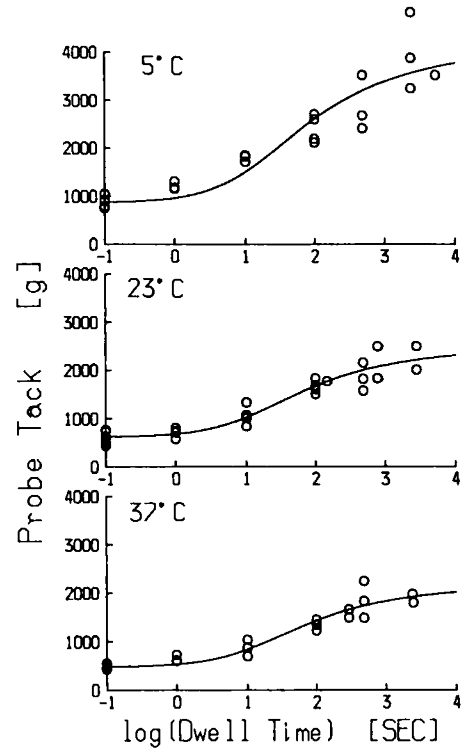

FIGURE 12 Probe track *vs.* dwell time for PSA-N. Solid line is a curve of the 4th order rate equation.

parameters obtained by this curve-fitting are not necessarily significant, because it is only an assumption that the rate of increase of the probe tack can be described by the *n* th order rate equation, and because there is scatter of the points.

However, it is expected that we obtain information about the difference in the rate of increase of the probe tack with time and temperature of the two PSAs in terms of the relative values of the parameters, especially the rate constant *k*. The Arrhenius plot of *k* is given in Figure 13 and the activation energy of the bonding process of PSA-T is 17 kcal/mole and that for PSA-N is 10 kcal/mole.

It is interesting to notice that ΔH^*_{bond} of PSA-T is larger than that of PSA-N, although the absolute values of both are rather small. Because the activation energy of the two PSAs in the lower part of the f *vs.* $\log v$ curve, where the debonding process is dominant, is 19 kcal/mole, the authors expected that ΔH^*_{bond} of PSA-N would be around 19 kcal/mole and that of PSA-T would be greater. The reason why the experimentally-obtained activation energies for the bonding process are somewhat smaller than our anticipation will be that the contacting process proceeds in the pulled state in case of the pulling cylinder test, while it proceeds in the pushed state in case of the probe tack test, and that the cylinder is

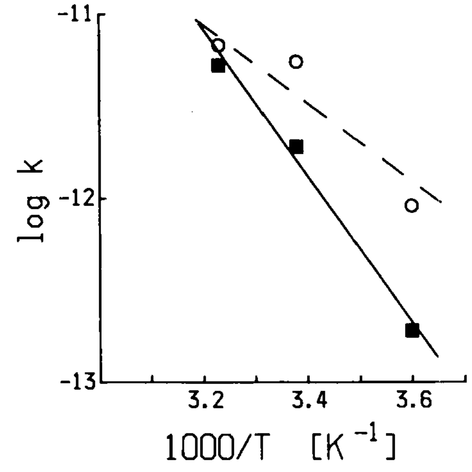

FIGURE 13 Arrhenius plot of the rate constant k of the bonding process for PSA-T and PSA-N. ○: PSA-N, $\Delta H^*_{\mathrm{bond}} = 10$ kcal/mole, ■: PSA-T, $\Delta H^*_{\mathrm{bond}} = 17$ kcal/mole.

brass, while the probe is stainless steel. Anyway, it is suggested here that $\Delta H^*_{\mathrm{bond}}$ of PSA-T is relatively larger than that of PSA-N.

CONCLUSIONS

Rolling friction coefficient of two PSAs (PSA-T and PSA-N) is measured by means of the pulling cylinder method at several temperatures. We find two peaks (or a peak and a shoulder) in every case, and when temperature is lowered, the curve shifts toward the lower velocity region. We have noticed that the time–temperature superposition procedure is not applicable to PSA-T, but it is applicable to PSA-N. Numerical calculations according to the theory which the authors have recently proposed lead us to the conclusion that $\Delta H^*_{\mathrm{bond}}$ is larger than $\Delta H^*_{\mathrm{debond}}$ in the case of PSA-T, and $\Delta H^*_{\mathrm{bond}}$ is almost equal to $\Delta H^*_{\mathrm{debond}}$ in the case of PSA-N. Then, probe tack of the two PSAs are measured as a function of dwell time at three temperatures. Analysis of the data according to the nth order equation for the rate of increase of the true contact area lead us to the conclusion that $\Delta H^*_{\mathrm{bond}}$ of PSA-T is larger than that of PSA-N.

It is quite reasonable that the two PSAs behave the same concerning the cohesive failure, and therefore $\Delta H^*_{\mathrm{debond}}$ of the two is almost the same, because they have the same chemical composition and the same molecular weight, and there can be no great difference in their bulk properties. However, the reason why the two PSAs can have different values of $\Delta H^*_{\mathrm{bond}}$ is not well known. One of the possibilities is that the releasing agent used in the PSA-T system was different from that in the PSA-N system, and that some amount of the releasing agents has transferred onto the surface of PSAs in a different manner for the two adhesives, which had some influence on the rate of the bonding process. If this is true, it is expected that the measurement of f in the high velocity region gives us information on the difference of the characteristics of the releasing materials. In conclusion, a quantiative explantion of the above-mentioned phenomena is not necessarily possible now, but it seems plausible that the time–temperature superposition principle is apparently applicable only in the case where ΔH^*_{bond} is equal to $\Delta H^*_{\text{debond}}$ in rolling friction of tack materials.

Acknowledgements

Part of the work was supported by a Grant-in-Aid of the Ministry of Education, Science and Culture of Japan. The authors wish to thank Toyo Ink Manufacturing Co., Ltd. and Nichiban Co., Ltd. for various aids.

References

1. F. Urushizaki, H. Yamaguchi and H. Mizumachi, *J. Adhesion Soc. Japan* **20,** 295 (1984).
2. H. Mizumachi, *Material Technology* (*Japan*) **2,** 6 (1984).
3. H. Mizumachi, *J. Adhesion Soc. Japan* **20,** 522 (1984).
4. H. Mizumachi and T. Saito, *J. Adhesion* **20,** 83 (1986).
5. H. Mizumachi, *J. Appl. Polym. Sci.* **30,** 2675 (1985).
6. H. Mizumachi and Y. Hatano, *J. Adhesion* **21,** 251 (1987).
7. W. M. Bright, in *Adhesion and Adhesives,* J. E. Rutzler, Jr. and R. L. Savage, Eds. (John Wiley and Sons, Inc., New York, N.Y., 1954), p. 130.
8. K. Kanamaru, *Kolloid-Z.* **192,** 51 (1963).
9. J. Furukawa, in *Adhesion and Lamination* (Soc. Polym. Sci. Japan, Ed.), p. 196.
10. Y. Hatano and H. Mizumachi, *J. Appl. Poly. Sci.,* in press.
11. T. Hata, *Zairyo* (*Materials*) **17,** 322 (1968).
12. T. Hata, *J. Adhesion Soc. Japan* **8,** 64 (1972), (*J. Adhesion* **4,** 16 (1972)).